XPCS at the Microsecond Frontier: Diffusion of PEGylated Nanoparticles in Water – Supporting Information

Nele N. Striker,[a] Florian Schulz[b], Claudia Goy[a], Jonathan Correa[a], Adriana Simancas[a], Francesco Dallari[c], Daniele Marzi[d], Randeer Pratap Gautam[a], Carlos Arauz-Moreno[f], Robert P.C. Bauer[a], William Chèvremont[d], Marco Cammarata[d], Heinz Graafsma[a], Frédéric Caupin[e], and Felix Lehmkühler*[a]

1 DLS Measurements

DLS measurements were performed with a Zetasizer Nano ZS system (Malvern Instruments), which employs a He–Ne laser (4.0 mW, 633 nm). Data were analyzed using Dispersion Technology Software (version 6.20). UV microcuvettes (Plastibrand, Carl Roth GmbH, Karlsruhe, Germany) were used with sample volumes of 200 μL. All samples were measured three times, and the discussed hydrodynamic radii are the centers of the volume-weighted distributions. The volume-weighted distributions are chosen because for citrate coated AuNP (the citrate ligand adds little to the hydrodynamic radii) these provided the best agreement with size distributions obtained by TEM analysis.

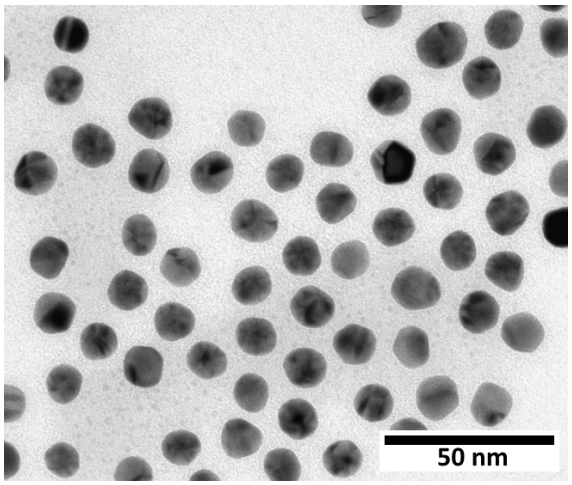

Fig. S1. Exemplary TEM micrograph of gold nanoparticles (AuNP) with a core radius $R_c = (6.1 \pm 1.2)$ nm. Sample AuNP5 in the main text.

2 Transmission Electron Microscopy (TEM)

TEM measurements were performed using a JEOL JEM-1011 electron microscope operating at 100 kV. Samples of AuNP@PEGMUA conjugates were prepared by pipetting approx. 10 μL of the sample onto carbon-coated copper grids, which were placed on a glass slide and allowed to dry for at least 24 h. Quantitative analyses of AuNP size distributions based on TEM measurements were performed using the software ImageJ (version 1.43u). The results are shown in Figs S1 and S2 . Note that core radii R_c are given, whereas in table 1 in the main text the hydrodynamic radii R_h are listed including the contributions of the ligand shells which are not discernible in TEM. The differences $R_h - R_c$ consistently yield an estimate of the thicknesses of the PEG shells of approx. 8 nm for PEGMUA2k and approx. 12 nm for PEGMUA5k in agreement with previous studies[1,2].

[a] *Deutsches Elektronen-Synchrotron DESY, Notkestr. 85, 22607 Hamburg, Germany*
[b] *Center for Hybrid Nanostructures, Universität Hamburg, 22761 Hamburg, Germany.*
[c] *Department of Physics and Astronomy "Galileo Galilei", University of Padova, Padova, Italy*
[d] *ESRF, The European Synchrotron, 71 Avenue des Martyrs, CS40220, 38043 Grenoble Cedex 9, France.*
[e] *Institut Lumière Matière, Université Claude Bernard Lyon 1, CNRS, Institut Universitaire de France, 69622 Villeurbanne, France.*
[f] *Université Grenoble Alpes, CNRS, LIPhy, 38000 Grenoble, France.*

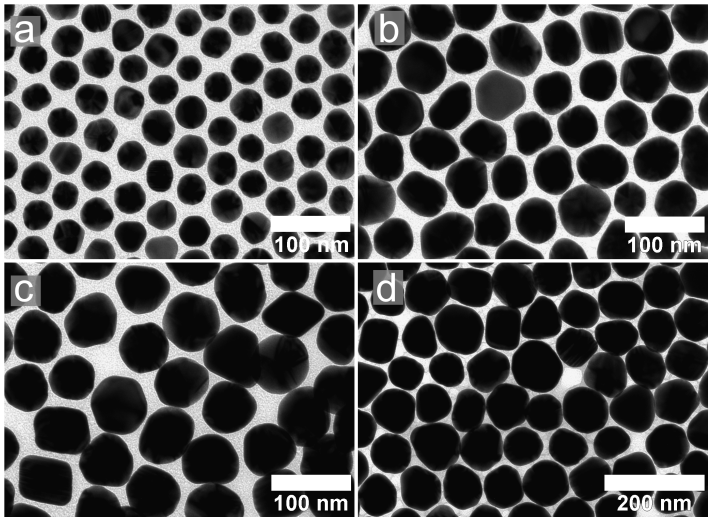

Fig. S2. Exemplary TEM micrographs of the bigger AuNP discussed in the main text. (a) AuNP1, $R_c = (18.8 \pm 3.1)$ nm. (b) AuNP2, $R_c = (28.1 \pm 2.8)$ nm. (c) AuNP3, $R_c = (32.9 \pm 4.9)$ nm. (d) AuNP4, $R_c = (41.1 \pm 3.7)$ nm.

3 Additional data for sample AuNP1

Here we show additional SAXS and XPCS data for sample AuNP1 measured at ID02 (ESRF). While in the main text the data is shown for the largest studied gold nanoparticles (AuNP4), we here show the same results for the smallest studied sample (AuNP1). Note that also this sample had 5 kDa PEGMUA ligands compared to 2 kDa of AuNP4. The data shown here is obtained from the lowest concentration of AuNP1 and thus shows the results with the most limited statistical accuracy.

Fig. S3 shows the $I(q)$ (panel a) and the square of the intermediate scattering function $|f(q,\Delta t)|^2$ (panel b) at $q = 0.004$ nm^{-1}. Compared to the data shown in the main text, the data is more affected by noise due to the reduced scattering power of the sample.

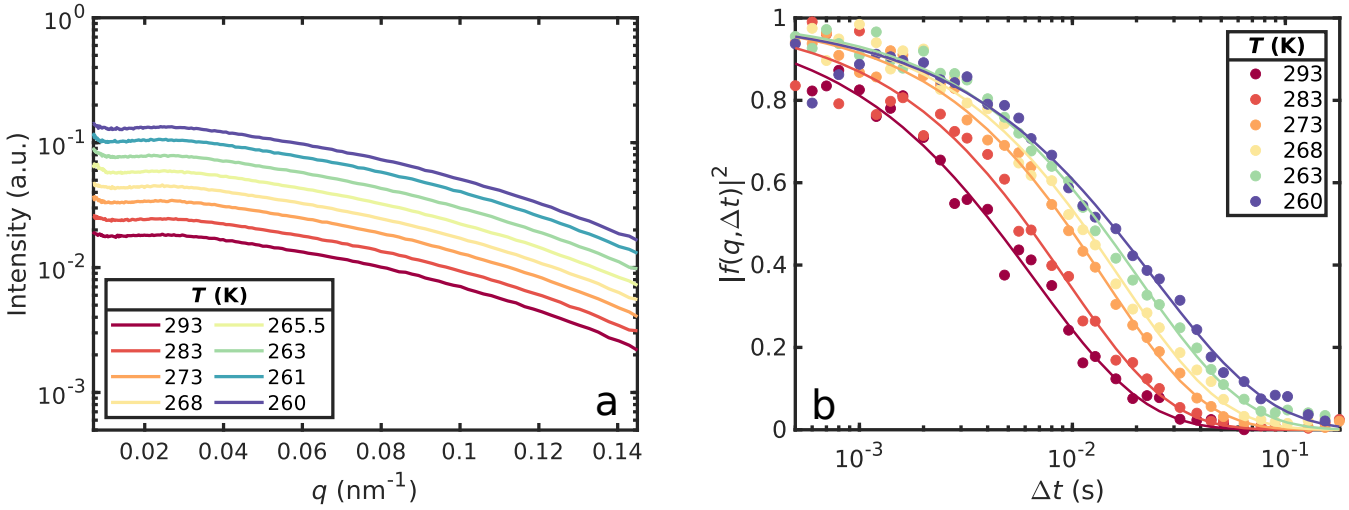

Fig. S3. (a) Azimuthally averaged scattered intensity of AuNP1 with 5 kDa PEGMUA ligands at $\phi = 0.0026$ for decreasing temperatures. The intensity profiles have been shifted vertically for clarity. (b) Modulus square of the intermediate scattering functions $|f(q,\Delta t)|^2$ at $q = 0.004$ nm^{-1} for the same sample and temperatures. The lines are fits with Eq. 3 of the main manuscript.

Fig. S4 (a) shows square of the intermediate scattering function $|f(q,\Delta t)|^2$ at different q values and fixed temperature $T = 293$ K. The resulting relaxation times τ are shown in Fig. S4 (b) together with the fit for diffusive dynamics.

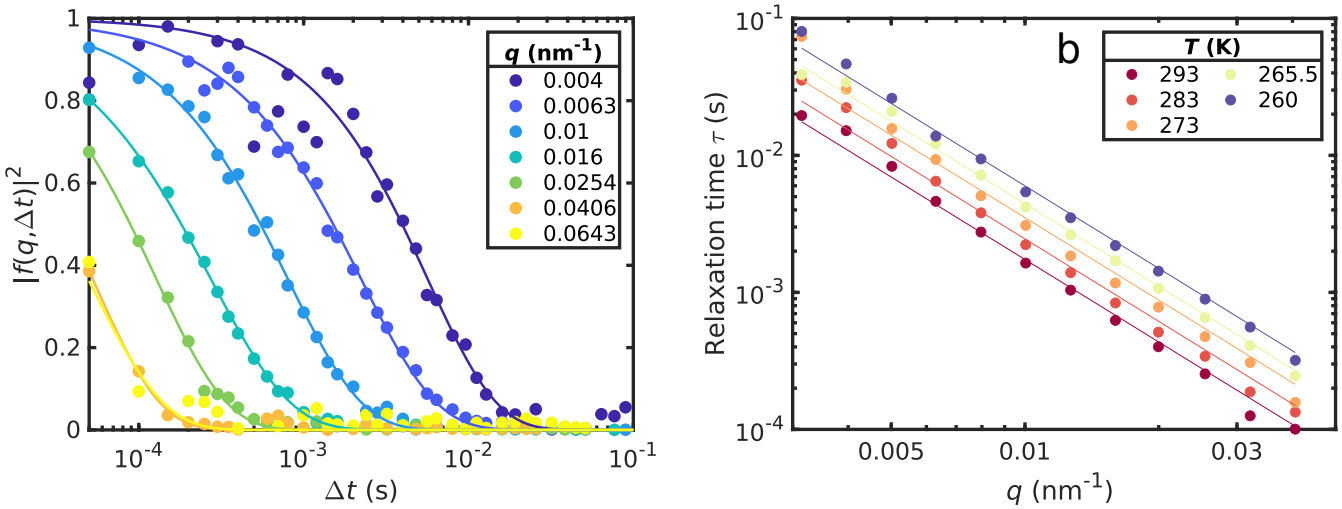

Fig. S4. (a) Modulus square of the intermediate scattering functions $|f(q,\Delta t)|^2$ at $T = 293$ K for sample AuNP1 with 5 kDa PEGMUA ligands at $\phi = 0.0026$ for different values of q. The lines are fits of Eq. 3 of the main manuscript to the data. (b) Relaxation times τ as a function of q at all measured temperatures T for sample AuNP1 with 5 kDa PEGMUA ligands. The lines correspond to fits of type $\tau = 1/D \cdot q^{-2}$.

4 Additional TEMPUS data

Additional XPCS data taken with the TEMPUS detector at beamline P10 of PETRA III is shown in this section. The XPCS data was taken for sample AuNP4 with 2 kDa ligands. The data shown in Fig. S5 was averaged from two XPCS exposures, each taking 30 s. An attenuated beam (transmission around 0.097) was used so that the sample was stable over the exposure time. The total data time of 60 s was below the data time taken at ESRF of 40 scans with 5s exposure each (leading to a total sample time of 200 s), and an attenuator setting leading to a transmission of about 0.02. Together with the different intensity at P10 and ID10 of about an order of magnitude more coherent flux at ID10 thanks to ESRF-EBS upgrade, this indicates the lower noise level of the ID10 data shown in the main text. Fig. S5 shows the extracted relaxation times of the TEMPUS data and compares them to the ID02 data taken from the same sample. This highlights the potential of TEMPUS for capturing faster dynamics and thus extending towards larger q for the present samples.

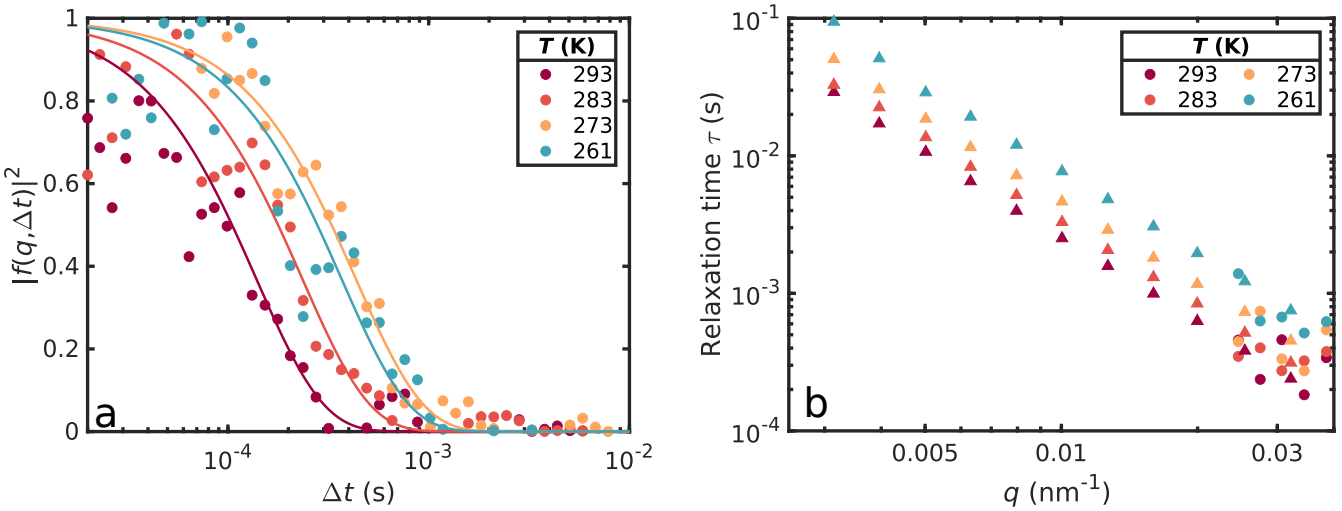

Fig. S5. a) Intermediate scattering functions $|q_1(q,\Delta t)|^2$ of sample AuNP4 with 2 kDa ligands for different temperatures measured with the TEMPUS detector at P10. Data is shown for $q = 0.0275$ nm^{-1}. (b) Relaxation times τ as a function of q for sample AuNP4 with 2 kDa ligands at different temperatures measured with TEMPUS at P10 (dots) and Eiger 500k at ID02 (triangles).

5 Residuals

The residuals, i.e., differences between the data points and the models from Figs. 3 b and 4 d are added below. The values from the model are subtracted from the experimentally obtained values. The residuals highlight the deviations at lower temperatures.

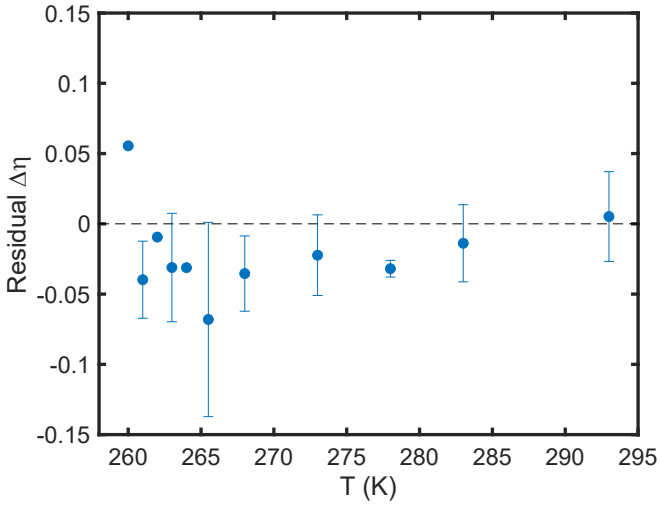

Fig. S6. Relative residual $\Delta\eta = (\eta_{exp} - \eta_{model})/\eta_{model}$ from the data shown in Fig. 3 b. Data points without error bars are obtained from single samples only.

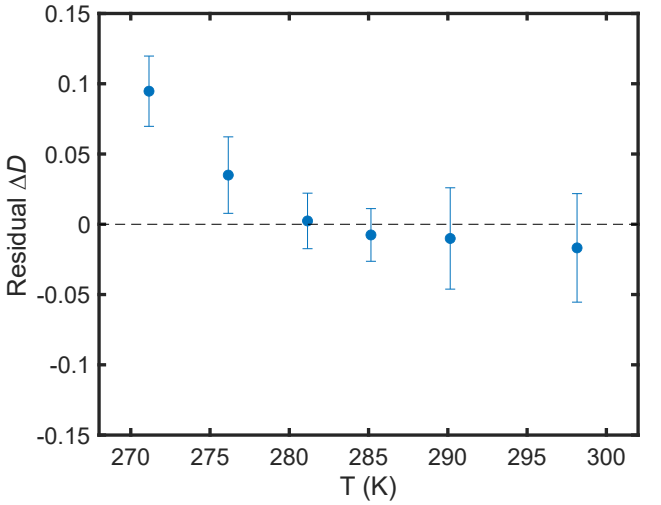

Fig. S7. Residual $\Delta D = (D_{exp} - D_{model})/D_{model}$ from the data shown in Fig. 4 d.

Notes and references

1 M. A. Schroer, F. Schulz, F. Lehmkühler, J. Möller, A. J. Smith, H. Lange, T. Vossmeyer and G. Grübel, *The Journal of Physical Chemistry C*, 2016, **120**, 19856–19861.

2 F. Schulz, J. Möller, F. Lehmkühler, A. J. Smith, T. Vossmeyer, H. Lange, G. Grübel and M. A. Schroer, *Part. Part. Syst. Char.*, 2018, **35**, 1700319.